AENSI Journals

Australian Journal of Basic and Applied Sciences

ISSN:1991-8178

Journal home page: www.ajbasweb.com

Automatic Authentication using Random Encoding based Cancelable Iris Template embedded in QR Code

[1]S. Brindha and [2]Dr. Ila.vennila

[1]*Senior Lecturer and HoD, Dept. of Computer Networking , PSG Polytechnic College, Coimbatore, India*
[2]*Associate Professor, Department of Electrical and Electronics Engineering, PSG College of Technology, Coimbatore, India*

ARTICLE INFO

Article history:
Received 19 August 2014
Received in revised form
19 September 2014
Accepted 29 September 2014
Available online 8 November 2014

Keywords:
Iris Recognition, Cancelable iris code, QR code, Biometrics, Mobile Ticket

ABSTRACT

Background: User authentication is a pivotal component of current security infrastructure. One of the major challenges in deploying biometric keys is improving user convenience and reducing identification time. By combining Quick Response (QR) codes and cancelable iris templates a new dimension in automatic user authentication is proposed. **Objective:** In this paper, an authentication method using cancelable iris template embedded in Quick Response codes is proposed. Automated iris recognition system using QR code is a relatively new technique for authentication. This scheme provides a non invasive and fast authentication for large population of users who can bring their nominative tickets in electronic form. This approach will be suitable for mobile ticketing applications. **Results:** The proposed cancelable iris embedded in Quick response codes approach was evaluated using 100 images taken from publicly available CASIA-IrisV3-Interval database. The performance improvement was observed using False Acceptance Rate (FAR) and False Rejection Rate (FRR) as the metrics. The experimental results also show an effective reduction in time taken for identify verification. **Conclusion:** The cancelable iris templates have been generated using random encoding of consistent bit vectors. The cancelable iris templates have been embedded in Quick Response codes and used for two factor authentication. Users can walk through the iris scanner and QR code scanner for authentication.

To Cite This Article: S.Brindha and Dr.Ila.Vennila., An Efficient Feature Extraction and Random Encoding based Cancelable Iris Template Generation Scheme for Automatic Authentication, ***Aust. J. Basic & Appl. Sci.,*** *8(17): 196-203, 2014*

INTRODUCTION

User authentication is done based on knowledge, possession or biometrics (Basavala *et al*. 2012). Iris recognition technology has revolutionized the field of biometrics by combining the unprecedented security of iris recognition with a quick, easy-to-use solution. Unlike other systems that require users to stop or to position their eyes close to a camera, iris authentication can be done on the move and enables people to simply glance and go regardless of lighting conditions, indoors or out and face expressions. Ideal for high-traffic applications such as airports and border crossings, this method of iris walk-through recognition has a processing speed of approximately 30 people per minute. Users can simply walk through at a comfortable pace. It is an effective solution for applications that require rapid identity verification of a large number of people. Quick response (QR) codes and iris are combined to provide a new two factor authentication scheme (Brindha *et al*. 2013).

Cancelable biometrics has been suggested by many researchers for protecting the templates. Non invertible transforms can be applied in image and feature domain. Rathgeb and Busch (2013) suggest to operate in image domain for iris codes. The annular iris shape is unwrapped into rectangular iris texture by Ma *et al*., (2003). This paper sets its focus on the security of a custom made iris recognition system based on the feature extraction algorithm of Jing *et al*. (2009) which is followed by a random encoding based cancelable iris template embedded in QR codes. QR codes are being used for authentication as indicated by Conde-Lagoa *et al*. (2010) and Dey et.al. (2013).

In the proposed iris recognition system, the set of pixels containing only the iris are extracted and normalized by Daugman's rubber sheet model to compensate for pupil dilation or contraction. The bit patterns are the extracted using random encoding. Iris recognition system mainly aims at extracting the iris features. A unified approach is required in the following five levels to arrive at the two factor authentication scheme based on bit patterns from iris and QR code.

Corresponding Author: S. Brindha, HoD, Department of Computer Networking, PSG Polytechnic College, Coimbatore, India.
E-mail:hod@dcn.psgtech.ac.in, Phone:+91-9442075445

Australian Journal of Basic and Applied Sciences, 8(17) November 2014, Pages: 196-203

Level 1: Segmentation
Level 2: Normalization
Level 3: Iris texture extraction
Level 4: Random encoding
Level 5: Embedding in QR code

1.1 Level 1:Segmentation:

Iris segmentation is an essential module in iris recognition because it isolates the actual iris from eye image. Iris segmentation consists of two phases 1) edge detection using wavelet function 2) iris boundary detection.

1.1.1 Edge detection using wavelet transform:

A non-separable wavelet transform as proposed by Jing *et al*. (2009) is used to extract the wavelet transform modulus of the iris image, and then radial non- maxima suppression is proposed to retain the annular edges and simultaneously remove the radial edges. Next, an edge thresholding is utilized to remove the isolated edges and determine the final binary edge map. Based on the binary edge map, iris boundary detection using Hough transform is done.

In the case of the iris segmentation, conventional edge detection methods not only detect the edges of iris boundaries, but also detect the noises, such as edges of eyelash, and edges of texture of iris. These noises are invalid to iris segmentation, and may result in the inaccuracy of iris segmentation. In order to detect high quality edge maps of iris images and segment irises accurately, a technique based on non separable wavelet transform is proposed.

A non-separable wavelet is constructed by using centrally symmetric matrices. The 4x4 centrally symmetric and orthogonal matrix U(α,β) defined as follows in Equation 1:

$$U(\alpha,\beta) = \frac{1}{2}\begin{pmatrix} \cos\alpha+\cos\beta & -\sin\alpha+\sin\beta & -\sin\alpha-\sin\beta & \cos\alpha-\cos\beta \\ \sin\alpha-\sin\beta & \cos\alpha+\cos\beta & \cos\alpha-\cos\beta & \sin\alpha+\sin\beta \\ \sin\alpha+\sin\beta & \cos\alpha-\cos\beta & \cos\alpha+\cos\beta & \sin\alpha-\sin\beta \\ \cos\alpha-\cos\beta & -\sin\alpha-\sin\beta & -\sin\alpha+\sin\beta & \cos\alpha+\cos\beta \end{pmatrix} \quad (1)$$

where α and β are arbitrary real numbers. From the above centrally symmetric matrix, a class of the non separable product wavelet filter is derived.

The low pass filter m_o (z1,z2) is defined as follows:

$$m_0(z_1,z_2) = \frac{1}{4}(1,z_1,z_2,z_1z_2)\left(\prod_{k=1}^{N} U_{(\alpha_k,\beta_k)}\, D(z_1^2,z_2^2)U_{(\alpha_k,\beta_k)}^T\right)V_0, \quad (2)$$
$$(z_1,z_2) \in \partial D \times \partial D,$$

where D={z:|z|≤1}, $\partial D = \{z: |z| = 1\}$ and three high pass filters with respect to the above low pass filter are as follows:

$$m_j(z_1,z_2) = \frac{1}{4}(1,z_1,z_2,z_1z_2)\left(\prod_{k=1}^{N} U_{(\alpha_k,\beta_k)} D(z_1^2,z_2^2)U_{(\alpha_k,\beta_k)}^T\right)V_j, \quad (3)$$
$$j = 1,2,3,$$

where

$$V_0 = (1,1,1,1,)^T, \quad V_1 = (1,-1,1,-1)^T, \quad V_2 = (1,1,-1,-1)^T, \quad (4)$$
$$V_3 = (1,-1,-1,1)^T.$$

$D(z_1,z_2)$ is the matrix of trigonometric polynomial below

$$D(z_1,z_2) = \begin{pmatrix} 1 & 0 & 0 & 0 \\ 0 & z_1 & 0 & 0 \\ 0 & 0 & z_2 & 0 \\ 0 & 0 & 0 & z_1z_2 \end{pmatrix}, \quad (z_1,z_2) \in \partial D \times \partial D. \quad (5)$$

In order to determine the rate of intensity change at each point in the iris image, the modulus of the wavelet transform is calculated. Assume that I*(x,y)* is an acquired iris image of size *M* * *N* pixels. At each scale *j* with *j>0* and $m_0^0 I = I(x,y)$, the non-separable wavelet transform decomposes image into a low pass band and $m_0^{j-1} I$ and three high pass bands and $m_1^j I, m_2^j I, m_3^j I$. Since the bands of the wavelet transform are used to find the edges, the wavelet decomposition is non-subsampled wavelet decomposition. Thus the four subbands are formed at the original image. The modulus of the non-separable wavelet transform can be computed by.

$$M^j I = \sqrt{|m_1^j I|^2 + |m_2^j I|^2}. \quad (6)$$

The pupillary center is estimated and edges are placed at the points with the local maximum module of wavelet transform. To further detect the edges of iris boundary and remove noises we perform hysteresis thresholding. The length of edge curve is calculated. If the length of edge curve is less than threshold Ti then the edge curve in final binary edge map is removed. By this way noise is removed.

1.1.2 Boundary Detection:

The inner iris boundary is detected using elliptical Hough transform. The outer iris boundary is detected using circular Hough transform. The classical Hough transform was concerned with the identification of lines in the image, but later, the Hough transform has been extended to identify positions of arbitrary shapes, most commonly circles or ellipses. From the edge map obtained, votes are cast in Hough space for the parameters of circles passing through each edge point. These parameters are the centre coordinates x and y, and the radius r, which are able to define any circle according to the Equation 6.

$$x^2 + y^2 = \mathrm{r}^2 \quad (7)$$

A maximum point in the Hough space will correspond to the radius and centre coordinates of the circle best defined by the edge points.

1.2 Level 2:Iris Normalization:

Normalization process involves unwrapping the iris and converting it into its polar equivalent. The rubber sheet model proposed by Daugman *et al*. 2004 is used. For every pixel in the iris, an equivalent position is found out on polar axes. The process comprises of two resolutions: Radial resolution, which is the number of data points in the radial direction and angular resolution, which is the number of radial lines generated around iris region. Using the following Equation 7, the iris region is transformed to a 2D array with horizontal dimensions of angular resolution and vertical dimension of radial resolution.

$$\mathrm{I}[\mathrm{x}(\mathrm{r},\theta), \mathrm{y}(\mathrm{r},\theta)] \rightarrow \mathrm{I}(\mathrm{r},\theta) \quad (8)$$

where, I (x, y) is the iris region, (x, y) and (r,θ) are the Cartesian and normalized polar coordinates respectively. The range of θ is [0 ,2π] and r is [0,1].x(r,θ) and y(r,θ) are defined as linear combinations set of pupil boundary points. The formulas given in the following Equation 8 perform the transformation.

$$\begin{aligned} x(r,\theta) &= (1-r)xp(\theta) + i(\theta) \\ \mathrm{y}(\mathrm{r},\theta) &= 1-\mathrm{r})\mathrm{y}_\mathrm{p}(\theta) + \mathrm{y}_\mathrm{i}(\theta) \\ \mathrm{x}_\mathrm{p}(\theta) &= \mathrm{x}_{\mathrm{p}0(\theta)+\mathrm{r}_\mathrm{p}\mathrm{Cos}(\theta)} \\ \mathrm{y}_\mathrm{p}(\theta) &= \mathrm{y}_{\mathrm{p}0(\theta)+\mathrm{r}_\mathrm{p}\mathrm{Sin}(\theta)} \\ \mathrm{x}_\mathrm{i}(\theta) &= \mathrm{x}_{\mathrm{i}0(\theta)+\mathrm{r}_\mathrm{i}\mathrm{Cos}(\theta)} \\ \mathrm{y}_\mathrm{i}(\theta) &= \mathrm{y}_{\mathrm{i}0(\theta)+\mathrm{r}_\mathrm{i}\mathrm{Sin}(\theta)} \end{aligned} \quad (9)$$

where $(\mathrm{x}_\mathrm{p}, \mathrm{y}_\mathrm{p})$ and $(\mathrm{x}_\mathrm{i}, \mathrm{y}_\mathrm{i})$ are the coordinates on the pupil and iris boundaries along the θ direction. $(\mathrm{x}_{\mathrm{p}0}, \mathrm{y}_{\mathrm{p}0})$ and $(\mathrm{x}_{\mathrm{i}0}, \mathrm{y}_{\mathrm{i}0})$ are the coordinates of pupil and iris centers.

1.3 Level 3: Extraction of Iris Texture:

The normalized 2D form image is broken up into 1D signal, and these signals are used to convolve with 1D Gabor wavelets. The frequency response of a Log-Gabor filter is given as in Equation 9,

$$\mathrm{G}(\mathrm{f}) = \exp\left(\frac{-(\log\left(\frac{\mathrm{f}}{\mathrm{f}_0}\right))^2}{2(\log(\sigma/\mathrm{f}_0))^2}\right) \quad (10)$$

where f_0 represents the centre frequency, and σ gives the bandwidth of the filter. The Log-Gabor filter outputs the biometric feature (texture properties) of the iris.

The texture properties obtained from the log-gabor filter are complex numbers (a + ib). Iris texture features are stored in two different vectors: Vector I_1 contains the real part of the complex numbers and Vector I_2 contains the imaginary part of the complex numbers as in Equation 10.

$$\begin{aligned} \mathrm{I}_1 &= [\mathrm{a}_1\mathrm{a}_2\mathrm{a}_3 \ldots \mathrm{a}_\mathrm{m}]; |\mathrm{I}_1| = \mathrm{m} \\ \mathrm{I}_2 &= [\mathrm{b}_1\mathrm{b}_2\mathrm{b}_3 \ldots \mathrm{b}_\mathrm{m}]; |\mathrm{I}_2| = \mathrm{m} \end{aligned} \quad (11)$$

Australian Journal of Basic and Applied Sciences, 8(17) November 2014, Pages: 196-203

1.4 Level 4: Random Encoding:

Cancelable biometrics refers to the intentional and systematically repeatable distortion of biometric features in order to protect sensitive user-specific data. If a cancelable feature is compromised, the distortion characteristics are changed, and the same biometrics is mapped to a new template, which is used subsequently.

A novel cancelable biometrics scheme for protecting iris codes using random encoding is proposed. The main advantage of this scheme is that no user-specific key/password needs to be associated with each user. Rather, the random sequence employed in the cancelable transformation process can be set common to all users. Hence, this random sequence can be stored centrally in the application database. In contrast with other existing methods, the feature transformation of the proposed method is non-invertible even if it is known to an attacker. Moreover, the recognition accuracy is preserved even if the same key is employed with all users. That is, the transformation key need not be kept unique or secret.

The proposed method consists of three stages: (1) consistent bits extraction (2) Mapping bits with random sequence and (3) cancelable code generation. As shown in **Fig 1**, at enrolment, three sample iris images are captured from the eye being enrolled and iris codes for the captured images are generated and collected in three binary vectors. Then, the most consistent bits are extracted from the three vectors and collected in a consistent bit vector C; and their positions, in the true iris codes, are collected in a position vector P. The most consistent bits are bits that have lower probability of flipping across iris codes generated from three samples of the same iris compared to other bits [5]. A bit is considered consistent if it does not change its value across the k binary vectors. Then, bits in C are randomly mapped to another set of bits to constitute the protected code. Finally, the position vector and the protected code are stored in a centralized storage rather than the original iris code which can be discarded safely. At verification, a single iris image is captured from the eye being verified and the true iris code is generated for it. Using position indices stored in P, the most consistent bits are extracted from the generated Iris Code and collected in a consistent bit vector C′.

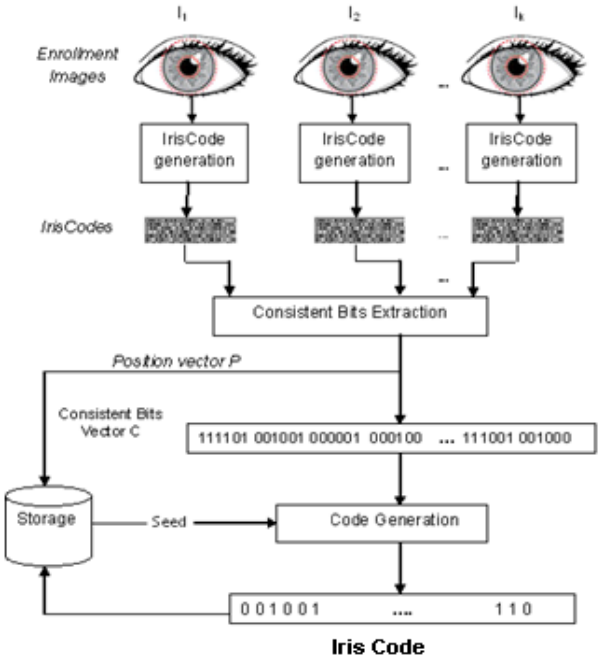

Fig. 1: Generating cancelable iris code.

Finally, the protected code for the eye being authenticated is derived from C′ and matched against the stored code.

1.5 Level 5: Embedding in QR code:

The QR barcode stores a considerably greater volume of information than a normal bar code. As shown in **Fig 2**, the three large squares act as alignment targets, while the smaller square in the remaining corner acts to normalize the size and angle of the shot. The strips near the alignment squares contain formatting information, and the remaining area is the actual data that is converted into binary code and checked for errors before being displayed. When a reader scans a symbol, it first detects these patterns. Once the position patterns have been detected the scanner can rapidly read the inside-code in all directions. The inside code consists of several small blocks where the information is encoded. The encoded data can be interpreted as one of four primary modes—numeric, alphanumeric, byte/binary, and Kanji. Other forms of data can also be displayed with appropriate extensions.

As QR code technology evolved, it began to contain more and more information. Specifically, its capacity can encode 7089 numeric characters for numeric data alone. The QR code has many desirable features like high capacity encoding of data, small printout size, Chinese/Japanese _kanji and kana_ capability, dirt and damage resistance, readability from any direction in 360º and a structure append feature. QR code can be easily generated using free on-line generators. They can be printed on plain paper and attached to any object.

Table 1: Levels of Iris feature extraction.

Level	Image
Input eye image	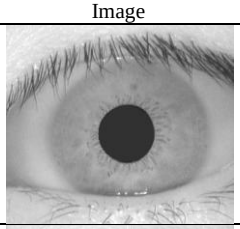
Locating the pupillary centre	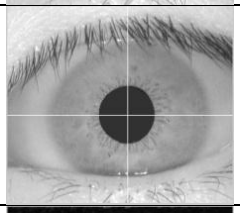
Edge Detection using modulus	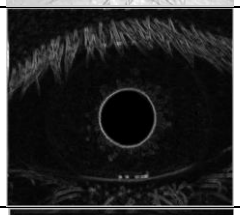
Noise removal	
Radial suppression	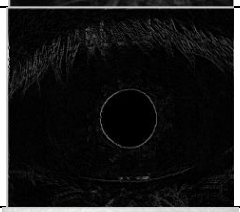
Boundary detection	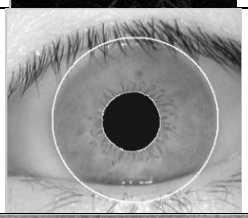
Unwrapped iris	
Cancelable iris code	0000010000000011000000100000001000000000010000011100 000010 00000011000000000000001110000011 000001110001 00111000001110000111000 00110000 00110000001100000011 00000 00110000111000000 11 1 11111000000000011000100000 00010010000000011 0 00 00 01000100 0 000010000000 00101

The 256 bit cancellable iris code is embedded in the QR code as shown in **Fig 2**. QR code is generated using Kaywa QR code generator. The various levels of feature extraction is shown in **Table1.**

2. Implementation:

In order to test the effectiveness of the proposed approach, experiments were conducted using iris codes embedded in QR codes. QR code was generated using online QR code generating software. The Kaywa QR

code generator was used in this experiment. The iris code is given as input and QR code of size 300*300 was generated.

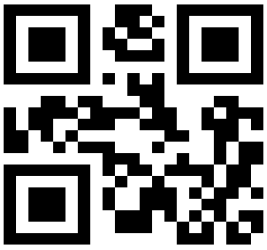

Fig. 2: Embedding iris bits in QR Code.

The generated QR code can be issued to the user as a nominative ticket. The publicly available iris image database collected by the Chinese Academy of Science-Institute of Automation, CASIA-IrisV3-Interval [2] was used in the experiments. This database contains 8-bit grayscale images with a resolution of 320 × 280 pixels. The iris code is generated using MATLAB implementation. The QR code decoding was implemented both in mobile phone and PC. The mobile phone used was Samsung Galaxy Duos mobile phone with android 4.0 operating system,1GHz processor and 512MB RAM. The Matlab code for matching the iris was done using Intel Core2 CPU, 1.86GHz processor, 1GB RAM. The Quick mark QR code decoding software was used for the above purpose.

As we are focusing our proposed authentication system for large population where users can bring their nominative tickets in any form i.e., either in paper or through their mobile phones, the QR codes can be decoded from various input forms using QR code reading software. The mobile ticketing system is shown in **Fig 3.**

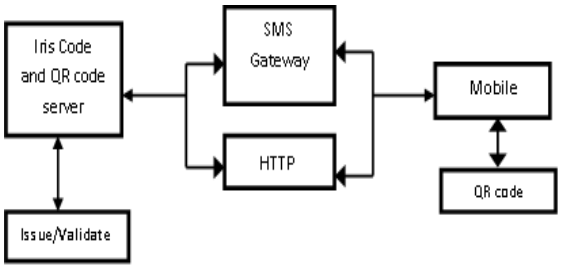

Fig. 3: Mobile ticket system.

Once the QR code is decoded the iris code will be obtained and then the user has to present him to the iris scanner where the iris image is scanned. The iris scanners available nowadays are able to capture the iris images when the users are on the move itself. Hence it will be convenient for the users to present their iris images. The scanned iris image is then converted into binary template and matched with iris code. If the matching is successful, the user will be authenticated.

3. Results:

The QR codes are scanned in PC using Quick mark QR code reading software. The scan time for various QR codes is shown in **Fig. 4**. The time taken for scanning QR codes is within 5 seconds per person. The time taken for authentication has been reduced in the proposed method. The metrics used for evaluation are False Acceptance rate (FAR) and False Rejection Rate (FRR). The FRR is the frequency that an authorized person is rejected access. The evaluation of iris recognition was carried out with 100 images taken from CASIA-IrisV3-Interval database, were grouped into ten users and the results are tabulated for FAR and FRR as in **Table 2. Fig 5** and **Fig 6** shows the resulted FRR and FAR as obtained from Equation 11, 12, 13 and 14 for the proposed cancelable iris code and existing true iris code technique.

$$\mathrm{FRR(n)} = \frac{\text{Number of rejected verification attempts for a qualified person n}}{\text{Number of all verification attempts for a qualified person n}} \quad (12)$$

$$\mathrm{FRR} = \frac{1}{\mathrm{N}} \sum_{\mathrm{n}=1}^{\mathrm{n}} \mathrm{FRR\,(n)} \quad (13)$$

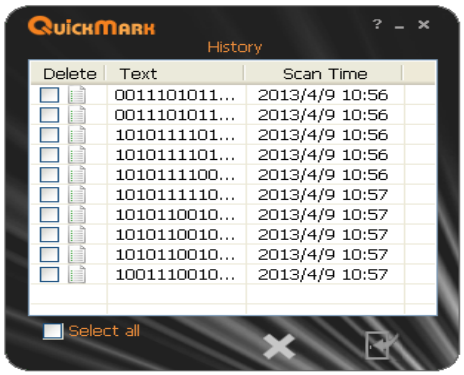

Fig. 4: Decoded QR code.

The FAR is the frequency that a non-authorized person is accepted as authorized.

$$FAR(n) = \frac{\text{Number of successful independent fraud attempts against a person n}}{\text{Number of all independent fraud attempts against a person n}} \quad (14)$$

$$FAR = \frac{1}{N}\sum_{n=1}^{n} FAR(n) \quad (15)$$

Table 2: FAR and FRR results.

No. of Users	FRR (%) for Iris	FRR (%) for Proposed Cancelable iris	FAR (%) for Iris	FAR (%) for Proposed Cancelable iris
1-10	88.7	87.7	0.35	0.33
11-20	87.9	87.9	0.33	0.31
21-30	89.1	89.5	0.37	0.37
31-40	88.5	88.9	0.39	0.38
41-50	88.9	89.2	0.36	0.35
51-60	89.3	89.7	0.33	0.32
61-70	88.6	88.9	0.35	0.36
71-80	89.4	89.4	0.39	0.38
81-90	88.1	88.6	0.38	0.37
91-100	88.2	88.5	0.36	0.35

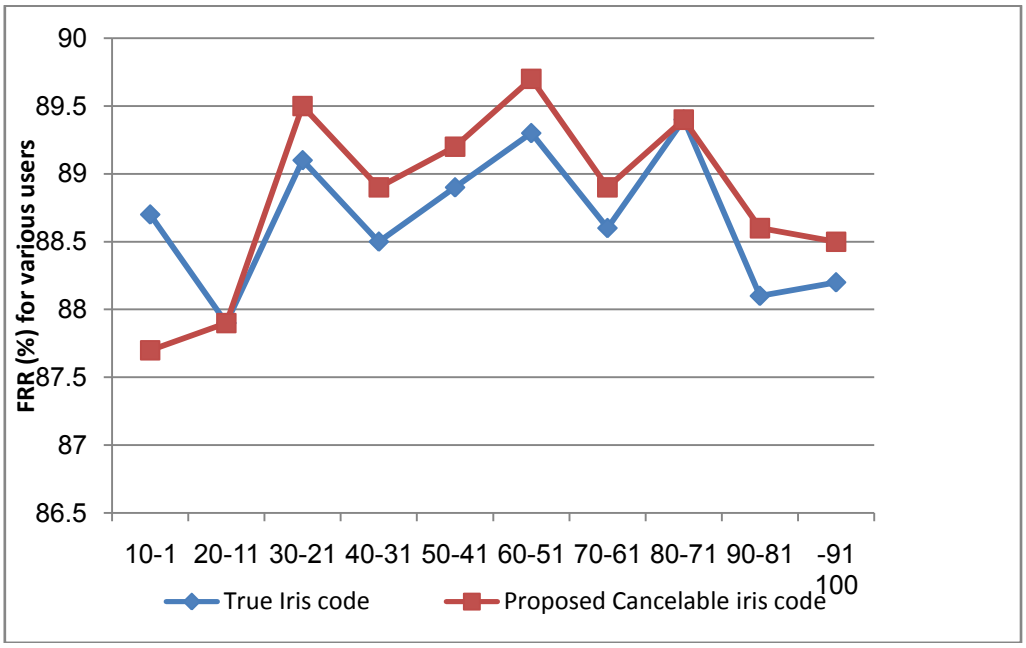

Fig. 5: Resulted False Rejection Rate.

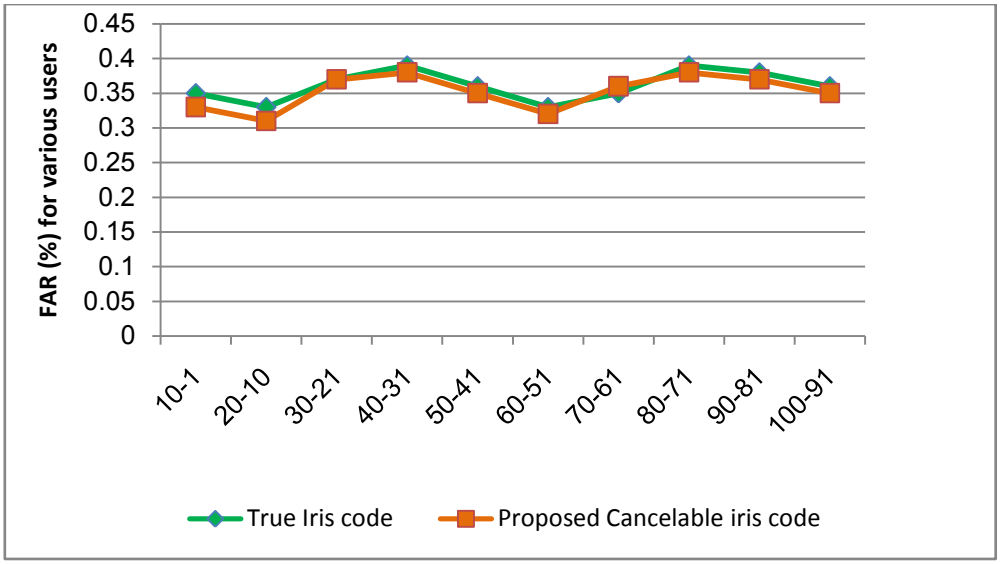

Fig. 6: Resulted False Acceptance rate.

4. Conclusion:

Biometrics and QR codes are combined to provide a two factor authentication where nominative tickets are required. The proposed model can be used for various applications. Automatic authentication is possible with state of art technologies like iris recognition on the move. As future improvement QR code can be encrypted and issued for enhancing security. In addition, from the view point of the service provider, no extra cost is necessary to create and maintain the database for storing each user's long-term secret key. There is no need to maintain a separate database file to verify the user's authentication request. The proposed iris recognition system is better than the other iris recognition approaches.

REFERENCES

Basavala S.R., N. Kumar and A. Agarrwal, 2012. Authentication: An overview, its types and integration with web and mobile applications, 2nd IEEE International Conference on Parallel Distributed and Grid Computing, Dec. 6-8, pp: 398-401. DOI: 10.1109/PDGC.2012.6449853.

Brindha, S., Ila.Vennila and B. Nivedetha, 2013. Secure User Authentication using Sclera in Quick Response Codes, *International Journal of Engineering and Technology*, 5(5): 4199-4205.

Conde-Lagoa, D., E. Costa-Montenegro, F.J. Gonzalez-Castao and F. Gil-Castiñeira, 2010. Secure eTickets based on QR-Codes with user-encrypted content. *Digest of Technical Papers International*, pp: 257-258. DOI: 10.1109/ICCE.2010.5418880.

Dey, S., A. Nath and S. Agarwal, 2013. Confidential Encrypted Data Hiding and Retrieval Using QR Authentication System, *International Conference on Communication Systems and Network Technologies*, April 6-8, pp: 512-517. DOI: 10.1109/CSNT.2013.112.

Jing Huang, Xinge You, Yuan Yan Tang, Liang Duand Yaun Yaun, 2009. A novel iris segmentation using radial-suppression edge detection, *Signal Processing*, 89(12): 2630-2643. DOI: 10.1016/j.sigpro.2009.05.001.

John Daugmann, 2004. How iris recognition works, *IEEE Trans. Circuits Syst. Video Technologies*, 141: 21-30. DOI: 10.1109/ TCSVT. 2003.818350.

Ma, L., T. Tan, Y. Wang, and D. Zhang, 2003. Personal identification based on iris texture analysis, *IEEE Transactions on Pattern Analysis and Machine Intelligence*, 1519-1533. DOI: 10.1109/TPAMI.2003.1251145 QR-Code Generator. http://qrcode.kaywa.com.

Rathgeb, C., C. Busch, 2013. Comparison Score Fusion Towards an Optimal Alignment for Enhancing Cancelable Iris Biometrics, *4th International Conference on Emerging Security Technologies*, Sept. 9-11, pp: 51-54. DOI: 10.1109/EST.2013.39.